Journal of Plant Diseases and Protection (2026) 133:94
https://doi.org/10.1007/s41348-026-01284-5

ORIGINAL ARTICLE

Predictive modeling of *Rhopalosiphum padi* population dynamics in time and space: host effects on management

Talison Roberto Maurer[1] · **Mateus Riva Donati**[1] · **João Pedro Moretti**[1] · **Jose Mauricio Cunha Fernandes**[2] · **Alexandre Tagliari Lazzaretti**[3] · **Roberto Wiest**[3] · **Crislaine Sartori Suzana-Milan**[1] · **Douglas Lau**[4] · **Rafael Rieder**[1]

Received: 23 September 2025 / Accepted: 3 May 2026

Abstract

The determination of biological parameters and the spatiotemporal dynamics of insect pests is essential for calibrating simulation models that enable the prediction of population growth and the establishment of warning systems for management actions. In this context, the objective of this study was to quantify variations in biological parameters due to the host (wheat cultivar) and their impacts on the accuracy of the ABISM (Agent-Based Insect Simulation Model). Since the rates of biological processes vary depending on the host plant, life-history parameters were obtained for two wheat cultivars (cv. TBIO Toruk and cv. BRS Belajoia) and compared to those simulated by ABISM. The pre-reproductive period was shorter, and longevity and the number of *R. padi* nymphs produced were higher in cv. BRS Belajoia compared to cv. TBIO Toruk. Differences were found between observed and ABISM-simulated data, depending on the cultivar, for the variables longevity ($p = 0.004793$) and total fecundity ($p = 0.04443$). These differences were expressed in spatial dynamics, with a greater number of plants colonized by *R. padi* in cv. BRS Belajoia. Differences between cultivars may be associated with anatomical traits, given that cv. BRS Belajoia lacks trichomes, unlike cv. TBIO Toruk. Therefore, there was an effect of cultivar and ambient temperature, and discrepancies between observed and simulated data only for cv. BRS Belajoia. The differences between cultivars, as well as in relation to the model, indicate, for better model accuracy, the use of cultivar-specific parameters considering insect–plant interactions is required.

Keywords Aphids · Insect–plant interactions · Predictive models · Plant resistance · Warning systems

---

✉ Rafael Rieder
rieder@upf.br

Talison Roberto Maurer
talismaurer@gmail.com

Mateus Riva Donati
182957@upf.br

João Pedro Moretti
183195@upf.br

Jose Mauricio Cunha Fernandes
jmauricio.fernandes@icloud.com

Alexandre Tagliari Lazzaretti
alexandrelazzaretti@ifsul.edu.br

Roberto Wiest
robertowiest@ifsul.edu.br

Crislaine Sartori Suzana-Milan
ssuzana@upf.br

Douglas Lau
douglas.lau@embrapa.br

[1] Universidade de Passo Fundo (UPF), BR 285 Km 292.7-Campus I-São José, Passo Fundo, RS, Brazil

[2] Independent Consultant, Passo Fundo, RS, Brazil

[3] Instituto Federal Sul-rio-grandense (IFSul), Estrada Perimetral Leste, 150-Parque Farroupilha, Passo Fundo, RS, Brazil

[4] Empresa Brasileira de Pesquisa Agropecuária (Embrapa), Estrada da Ribeira, Km 111-Parque Monte Castelo, Colombo, PR, Brazil

Introduction

Wheat and other winter cereals are the primary crops cultivated during the winter season in humid subtropical regions (Hernandez-Ochoa and Asseng 2018). Aphids are among the key pests that compromise grain yield in these cereals. In South America, *Rhopalosiphum padi* (Linnaeus, 1758) is recognized as one of the most economically important aphid species (Wiest et al. 2021).

R. padi is a significant pest that affects multiple crops. In addition to feeding on plant sap, this species transmits phytoviruses responsible for yellow dwarf disease in winter cereals, including barley yellow dwarf virus (BYDV) and cereal yellow dwarf virus (CYDV) (Parizoto et al. 2013; Aradottir and Crespo-Herrera 2021; Lau et al. 2021b, 2022). The extent of damage caused by *R. padi* depends on the cultivar and the phenological stage of the crop (Leather and Dixon 1981; Savaris et al. 2013).

As with other insects, environmental conditions and the host plant play a decisive role in shaping the life-history parameters of *R. padi*. Due to their ectothermic nature, aphids are highly affected by ambient temperature in their physiological processes. Temperatures between 20°C and 25°C are optimal for the development of this species (Villanuevab and Strong 1964; Auad et al. 2009; Strażyński and Ruszkowska 2015; Pds et al. 2016; Peng et al. 2017; Wiest et al. 2021). Beyond the thermal sum—defined as the accumulation of degree-days above a biological threshold—the temperature regime also shapes this insect's biology. For instance, a cyclic regime with a 10°C daily amplitude resulted in lower population growth compared to constant temperatures with equivalent degree-days (Wiest et al. 2021). Since daily thermal amplitude fluctuates under field conditions, these variations may lead to significant discrepancies when applying models calibrated under stable, controlled environments (Wiest et al. 2021).

Regarding the host factor, there may be variations among host plant species, as well as intraspecific variations due to genotype resistance. In Triticum species, partial resistance to *R. padi* has been reported (Hesler 2005; Peruzzo et al. 2007; Savaris et al. 2013; Girvin et al. 2017; de Jesus et al. 2020; Aradottir and Crespo-Herrera 2021; Simon et al. 2021). In some genotypes, lower preference, reduced reproduction (Razmjou et al. 2012), and negative effects on insect weight and survival have been observed (Singh et al. 2020). For instance, in trials comparing wheat phenological stages and cultivars, cv. BRS Timbauva exhibited lower population growth of *R. padi* and reduced yield loss than cv. Embrapa 16, suggesting antibiosis-type resistance (Savaris et al. 2013). Regarding the mechanisms involved in wheat resistance to *R. padi*, studies have demonstrated changes in gene expression profiles and metabolites (Batyrshina et al. 2020), as well as possible morphological factors such as trichomes contributing to resistance (de Jesus et al. 2020).

In terms of population dynamics, wheat cultivars resistant to *R. padi* have the potential to reduce aphid population growth and dispersal, thereby decreasing both direct and indirect damage to grain yield through BYDV transmission (Girvin et al. 2017). As yield loss is directly related to the number of plants infested by aphids and infected by the virus, predicting the spatial dynamics of aphids is crucial for forecasting and warning systems guiding management decisions.

Since aphid population dynamics are influenced by environmental factors, host plant resistance, and natural enemies (Brabec et al. 2014; D'agostini 2021; dos Santos et al. 2022; Engel et al. 2022; Santos-Cividanes et al. 2022), these variables must be systematically incorporated into models to reliably predict population growth. BYDV PREDICTOR is an example of a model developed to forecast aphid outbreaks and BYDV epidemics in wheat crops in southwestern Australia (Thackray et al. 2009). Based on daily precipitation and mean temperature data, it predicts the accumulation of *R. padi* during each winter cereal growing season and its migration into crops. This information is incorporated into farmers' decisions regarding insecticide applications (Thackray et al. 2009).

Another example is the ABISM (*Agent-Based Insect Simulation Model*), which is a generic model parameterized based on the life cycle characteristics of *R. padi* (Wiest et al. 2021). The system generates an aphid agent and simulates its life cycle in daily steps that consider the accumulated degree-days (°C day) required for development, reproduction, and age-related mortality. The model also applies daily rules for movement and mortality due to other factors, such as precipitation and natural enemies. ABISM is composed of the following modules: "Experiment", "Weather Data", "Field", and "Pest".

The "Experiment" module serves as a database and record of the simulations. The "Meteorological Data" module allows for the input of weather variables, either through manual entry or by retrieving information from stations that monitor temperature, precipitation, relative humidity, and other factors. The "Field" module simulates the area in which insect population dynamics develop and includes measurements of the area and number of host plants. The "Pest" module is responsible for the interaction between the insect and the environment. It stores data for each insect (agent) to determine its behavior (Wiest et al. 2021).

Daily development and reproduction of aphids are determined using equations proposed by Logan et al. (1976); Barlow and Dixon (1980); Morgan (2000). Parameterization is performed through degree-day weighting converted into a developmental scale. To estimate the duration of each developmental stage, degree-day weights were iteratively adjusted until simulated data closely matched observed data. Originally, the model was parameterized under a constant temperature regime using wheat cv. Embrapa 16 (Wiest et al. 2021).

In this context, we hypothesize that host-driven variations in *R. padi* life-history traits—measured at the individual level—scale up to significantly alter the spatiotemporal population dynamics and the predictive accuracy of simulation models. Specifically, we expect that accounting for these biological differences between wheat cultivars is essential for the ABISM model to reliably simulate pest outbreaks and support management decisions.

Materials and methods

Research site and plant material

We conducted the trials in controlled-environment plant growth chambers and screen houses at Embrapa Wheat, in Passo Fundo, Brazil (lat. −28.229804, long. −52.403555).

We used two wheat cultivars: BRS Belajoia (moderately tolerant to BYDV-PAV) and TBIO Toruk (moderately intolerant to BYDV-PAV) (Lau et al. 2021a).

Biological parameters of *Rhopalosiphum padi*

Experiments were performed in custom-built masonry growth chambers at 20±1°C with a 12:12 h (light/dark) photoperiod provided by 20 W LED lamps (6500 K; P.F. > 0.92). Initially, in a greenhouse, seeds of the two cultivars treated with the fungicide triadimenol (150 g/L) were sown in 1.5 L pots containing fertilized soil, following technical recommendations for fertilization and liming for wheat cultivation (Joris et al. 2022). We sowed six wheat seeds per pot and left three plants after thinning. Two weeks later, we transferred the plants to a controlled-environment growth chamber, where we initiated aphid infestation and conducted the trial.

To produce aphids for infestations, we initially selected 100 adult *R. padi* from colonies reared in an insectary. After 24 h, we removed the adults, leaving only the nymphs. After 5 days at 22°C with a 12:12 h photoperiod, aphids were used to infest plants at phenological stage 1.3, according to the scale of Zadoks et al. (1974) (Fig. 1A). One individual was placed per "clip cage" to confine it (Fig. 1B). The cage was considered the experimental unit of the trial. After 24 h, we removed the adults, and one nymph per cage was selected and observed until the end of its life cycle. During the first two weeks, if a nymph died (up to about six days

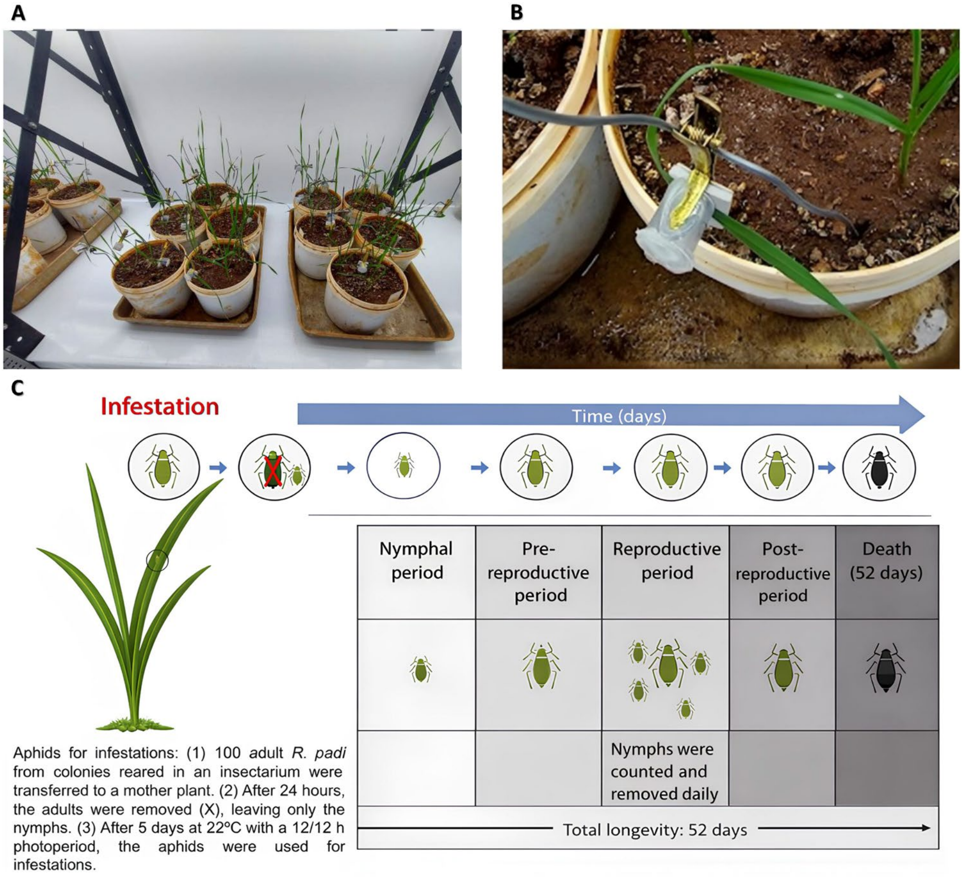

Aphids for infestations: (1) 100 adult *R. padi* from colonies reared in an insectarium were transferred to a mother plant. (2) After 24 hours, the adults were removed (X), leaving only the nymphs. (3) After 5 days at 22ºC with a 12/12 h photoperiod, the aphids were used for infestations.

Fig. 1 Experimental setup for the rearing, infestation, and determination of life history parameters of *Rhopalosiphum padi*. **A** Plants were maintained under controlled conditions (22°C and a 12:12 h (L:D) photoperiod) and infested at phenological stage 1.3, according to the Zadoks scale. **B** Detail of the clip cage used to confine a single aphid per plant. **C** Schematic representation of the experimental setup and life-history evaluation of *Rhopalosiphum padi*—adults were removed after 24 h, one nymph per cage was selected, and individuals were monitored throughout their life cycle after infestation), the dead individual was replaced, repeating the infestation procedure described above.

We calculated nymphal survival as the proportion of individuals that reached the reproductive stage relative to the total number of infested (including replaced) aphids. Daily observations tracked the progression through the nymphal stage, the age at which adults emerged, the number of offspring produced per adult per day, the duration of the reproductive period, and the time of death (Fig. 1C). The experiment lasted 52 days, ending with the death of the last aphid.

The following operational definitions were adopted for the life table analyses: pre-reproductive period was operationally defined as the cumulative duration of the nymphal stage and the subsequent pre-reproductive phase, representing the total time from birth to first reproduction; reproductive period was determined as the duration between the first and last nymph produced by each female; post-reproductive period comprised the time from the last offspring until death; longevity was defined as the total lifespan from birth to death; total fecundity corresponded to the total number of nymphs produced per female; and (daily) specific fecundity was calculated as the mean number of nymphs produced per female per day during the reproductive period.

To determine the appropriate statistical analyses, data were tested for normality using the Shapiro–Wilk test (Shapiro and Wilk 1965) and for homogeneity of variances by visual inspection of residual plots. Life-history variables that did not meet normality assumptions were analyzed using the nonparametric Kruskal–Wallis test (Kruskal and Wallis 1952), which does not require normally distributed data or homogeneity of variances. We compared the life table data obtained for each cultivar, along with other population parameters described below, to the values predicted by the ABISM model under a fixed temperature regime of 20°C, using the parameters defined by Wiest et al. (2021).

We calculated the relationship between thermal sum (accumulated degree-days) and aphid development for each cultivar. To determine the thermal sum, data on Experimental Temperature (T_e) and Basal Developmental Temperature (T_b) of *R. padi*, defined as 3.97°C (El-Fatih et al. 2015), were used, according to Equation 1:

$$T_d = T_e - T_b \tag{1}$$

The Developmental Temperature (T_d) was multiplied by the sum of days (D), generating the Thermal Sum (T_{Sum}) for each individual in the experiment, as shown in Eq. (2):

$$T_{\mathrm{Sum}} = \sum_{i=0}^{D} T_d \tag{2}$$

To generate the thermal sum graph using the mean data obtained for each cultivar, the "Tidyverse" package (Wickham et al. 2019) and "ggplot2" (Wickham 2016) in RStudio software (R Core Team 2024) were used. We compared the data with the thermal sum by developmental stage predicted by the ABISM model (Wiest et al. 2021).

To generate the reproduction and survival probability curves, we recorded the number of reproductive and living individuals daily, as well as their decline over time. We employed a binary coding system in which individuals were recorded as 0 (reproductive/alive) and coded as 1 when reproduction ceased or death occurred. To construct the probability curves, we used time as a covariate, tracking reproduction and survival rates until extinction. We performed all analyses in RStudio with the "survminer" package (Kassambara et al. 2021), along with the previously cited "Tidyverse" and "ggplot2" packages.

Survival analyses were conducted using Kaplan–Meier estimators (Kaplan and Meier 1958), which are appropriate for time-to-event data, particularly in the presence of censored observations, and do not assume a specific distribution of survival times. The survival function $S(t)$ estimates the probability that an individual survives beyond a given time t, with each time point corresponding to an observed event (e.g., death). The Kaplan–Meier curve was constructed as a stepwise function, in which survival probabilities are updated at each event as the product of preceding probabilities, according to the formula presented in Eq. (3). Differences among survival curves were assessed based on confidence interval overlap and model-based comparisons.

$$S(t) = \prod_{i=1}^{t} \left(1 - \frac{d_i}{n_i}\right) \tag{3}$$

where d_i is the number of events (deaths) at t_i, and n_i is the number of individuals at risk immediately before time t_i.

Population growth and dispersal

To obtain dispersal parameters of *R. padi* in two wheat cultivars, we conducted a trial under protected-environment (screen house) conditions at Embrapa Wheat in Passo Fundo, RS, Brazil. We arranged the experiment in a randomized block design with four replications. The sources of variation were cultivar (BRS Belajoia and TBIO Toruk) and infestation period (four levels), resulting in 32 experimental units. The experimental unit was a plastic tray with a capacity of 30 liters (62 × 14 × 36 cm). We filled the trays with soil-based substrate following technical recommendations for fertilization and liming for wheat cultivation (Joris et al. 2022). In each tray, we sowed 88 plants, distributed in 4 parallel rows, with each row consisting of 22 plants (Fig. 2A). Sowing took place on July 18, 2023, in mid-winter.

We conducted infestations at 14, 21, 28, and 35 days after sowing. We infested each tray with eight viruliferous *R. padi* individuals (carriers of BYDV-PAV), which we collected from cages containing black oat (*Avena strigosa* Schreb) plants. The aphids were adults of unknown age. Therefore, the initial population represented approximately 10% of the plants. Aphids were distributed across the four rows, with two individuals per row, positioned on the fourth and eighteenth plants (Fig. 2B).

After infestation, we protected the trays with a box-shaped structure covered on all sides with voile fabric to prevent aphids from escaping or being attacked by natural enemies. The duration of each infestation was 14 days. At the end of this period, we evaluated each plant individually and categorized it as follows: 0 = absence of aphids, 1 = presence of one aphid, and 2 = presence of more than one aphid.

For each treatment (cultivar × infestation period), we generated diagrammatic representations of plant colonization probability. For this purpose, we calculated the mean category of each plant position across the four treatment replications, classifying the plants into infestation probability classes ranging from 0% (no infestation) to 100% (high infestation).

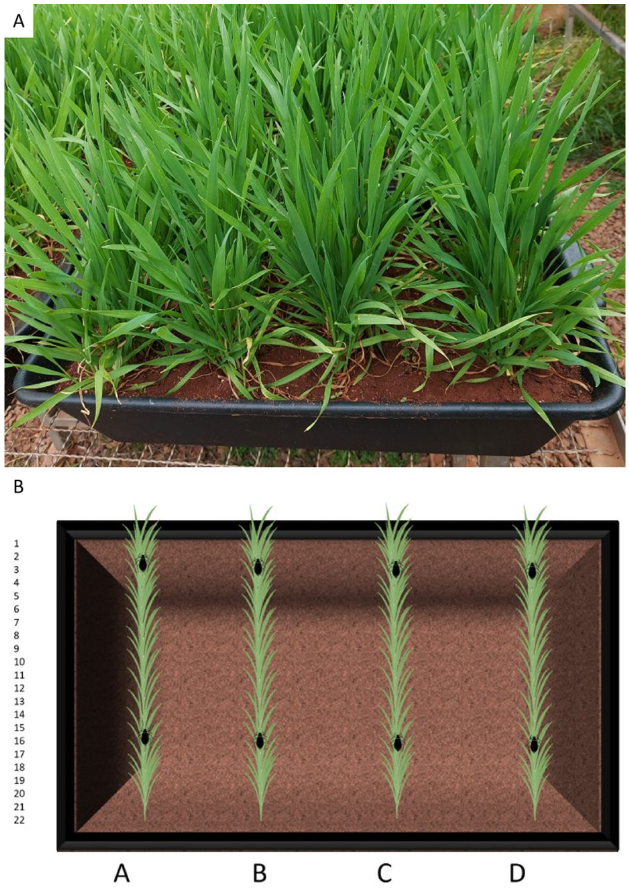

Fig. 2 Microplots for the analysis of aphid spatial distribution. **A** Photograph of the microplot. **B** Diagrammatic representation of the microplot, with four rows (**A**–**D**) and 22 plants each

We recorded daily maximum and minimum temperatures using an analog thermometer. The mean temperature for each infestation period was calculated and used as a parameter in the analyses and simulations in the ABISM model. In addition to temperature, we defined the configuration of the infestation area, the infestation density, and the aphid life parameters for the simulation.

We configured the "Field" module to have a single "MicroArea", corresponding to the experimental unit of one square meter. Immigration, emigration, and precipitation were disabled in the "MicroArea" module. We configured "MicroArea" with five rows of 60 plants each, totaling 300 plants/m^2. In "Host", the selected cultivar was Embrapa 16. The sowing date for the simulation was July 18, 2023, with the first simulated infestation date on August 1. The other simulated infestation dates were August 8, 15, and 22, successively, and simulations always lasted 14 days. In the "Weather Data" module, we selected the fixed data option, and the simulations considered the mean temperature of each period, with temperature values of 20°C, 21°C, 22°C, and 23°C (Wiest et al. 2021).

In the "Pest" module, under "Development", we defined the following indices: nymph (0–1.1), pre-reproductive (1.1–1.16), reproductive (1.16–2.3), post-reproductive (2.3–2.6), and death (2.6). The initial pests were introduced on plant 185 within the "MicroArea", in the adult, apterous, reproductive stage, with an initial accumulated temperature of 1.7 and five days of age. The initial number of pests was 30 individuals (equivalent to 10% of plants with aphids). Mortality due to parasitism, predation, low temperatures, and precipitation was disabled.

For graphical visualization and interpretation of the results, simulations were performed at 5°C intervals from 5°C to 20°C and at 1°C intervals from 21°C to 25°C. All statistical analyses were conducted in RStudio. Data normality was initially assessed using the Shapiro–Wilk test, and, after confirming approximate normality of residuals, a Linear Mixed-Effects Model (LMER) was applied using the "lme4" package (Bates et al. 2015). The model considered temperature as a random effect to account for variability among experimental conditions, as specified in Eq. (4). When significant effects were detected, differences between means were evaluated using Tukey's test at a 5% significance level, implemented via the glht function from the "multcomp" package (Hothorn et al. 2008). Graphs were generated using the "ggplot2" package.

$$\begin{aligned}&\text{Percentage of Plants with Aphids}_i\\&\quad\sim N\Big(\alpha_{j[i]} + \beta_1\,\text{Treatment}_{\text{TBIO Toruk}}\\&\qquad + \beta_2\,\text{Treatment}_{\text{ABISM}},\ \sigma^2\Big)\\&\alpha_j \sim N\Big(\mu_{\alpha_j},\ \sigma^2_{\alpha_j}\Big),\qquad \text{for Temperature } j = 1, \ldots, J\end{aligned} \tag{4}$$

Scanning electron microscope analysis

For the analysis of leaf epidermis by scanning electron microscope (SEM), we collected two leaves from each cultivar and subjected them to a dehydration process.

Initially, we fixed the leaves in FAA (ethyl alcohol, glacial acetic acid, formalin) 70% for 48 h at room temperature. We then transferred them sequentially to ethanol solutions of increasing concentration: 70% for two hours, 80% for two hours, 90% for two hours, 100% for 12 h, and 100% for an additional 12 h.

Subsequently, we immersed the leaves in ethanol–xylene mixtures at ratios of 3:1, 1:2, and 1:1, each for 2 h. Finally, we transferred the leaves to pure xylene and kept them there for two hours. We then subjected the samples to gold sputter coating and observed them under SEM (TESCAN©, VEGA model) at 1000× magnification.

Results

Biological parameters of *Rhopalosiphum padi*

The establishment and survival rate of nymphs was higher in cv. BRS Belajoia (93%) compared to cv. TBIO Toruk (70%). We carried out reinfestations and calculated the life table parameters for individuals that reached the reproductive period (Table 1).

Corroborating the hypotheses of this study, there were differences between the two cultivars in the duration of the pre-reproductive period, longevity, and total fecundity. The pre-reproductive period was shorter, and longevity and the number of nymphs produced were higher in cv. BRS Belajoia compared to cv. TBIO Toruk. However, the reproductive period and (daily) specific fertility (nymphs/female/day) did not differ between cultivars.

In comparison with the life parameters obtained in the present study, the current calibration in ABISM reproduces an aphid life cycle that is more closely aligned with that observed for *R. padi* developing on cv. TBIO Toruk.

In terms of thermal sum (accumulated degree-days, ° C day), the pre-reproductive period accumulated between 115.4°C day for cv. BRS Belajoia and 134.7°C day for cv. TBIO Toruk, whereas the current ABISM parameters estimate an accumulated 112.2°C day to complete this developmental stage. During the reproductive period, cv. BRS Belajoia accumulated 298.2°C day and cv. TBIO Toruk 270.9°C day, while the ABISM model accumulated only 176.3°C day for this phase.

The most significant differences in accumulated degree-days required to complete the developmental stages on each cultivar occurred during the post-reproductive period. Cv. BRS Belajoia showed the highest accumulation (185.9°C day), while cv. TBIO Toruk accumulated only 60.9°C day, resulting in a 125.0°C day difference between the cultivars. In comparison with ABISM (48.1°C day), the thermal sum was closer to that obtained for cv. TBIO Toruk, with only a 12.8°C day difference. Completing the entire life cycle required 599.5°C day for cv. BRS Belajoia, 466.5°C day for cv. TBIO Toruk, and 336.6°C day in the ABISM model (Fig. 3).

Specific fertility was higher during the first 14 days of the reproductive period in cv. BRS Belajoia (Fig. 4). After this period, cv. TBIO Toruk exhibited slightly higher fertility.

Table 1 Life table parameters of *Rhopalosiphum padi* on two wheat cultivars under controlled conditions (20±1°C, 12 h photoperiod) compared to the life cycle simulated by the ABISM model

Cultivars	n[A]	Pre-reproduc-tive period (days)[B]	Reproduc-tive period (days)[C]	Longevity (days)[D]	Fecundity nymphs/ female[E]	Specific fertility nymphs/ female/ day[F]
BRS Belajoia	37	7.2±0.1 b[G]	18.6±1.0 a[G]	37.4±1.4 a[G]	70.7±5.0 a[G]	4.1±0.3 a[G]
TBIO Toruk	39	8.4±0.2 a	16.9±1.1 a	29.1±1.4 b	50.9±3.2 b	3.5±0.3 a
CV(%)		17.6	37.7	28.6	45.1	47.9
ABISM		7.0	11.0	21.0	36.0	3.3

[A] Number of individuals used in the analysis

[B] Pre-reproductive period was operationally defined as the cumulative duration of the nymphal stage and the subsequent pre-reproductive phase, representing the total time from birth to first reproduction

[C] Reproductive period was defined as the duration between the first and last nymph produced by each female

[D] Longevity was defined as the total lifespan from birth to death

[E] Fecundity (total) corresponded to the total number of nymphs produced per female

[F] Specific fecundity was calculated as the mean number of nymphs produced per female per day during the reproductive period

[G] Kruskal–Wallis test at 5% significance; different letters indicate significant differences between cultivars

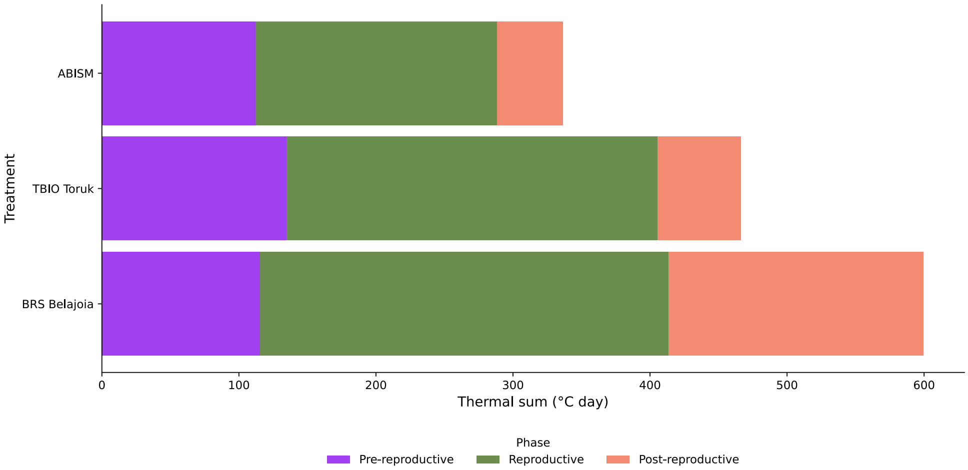

Fig. 3 Distribution of developmental phases of *Rhopalosiphum padi* on two wheat cultivars and simulated by ABISM in relation to thermal sum (accumulated degree-days)

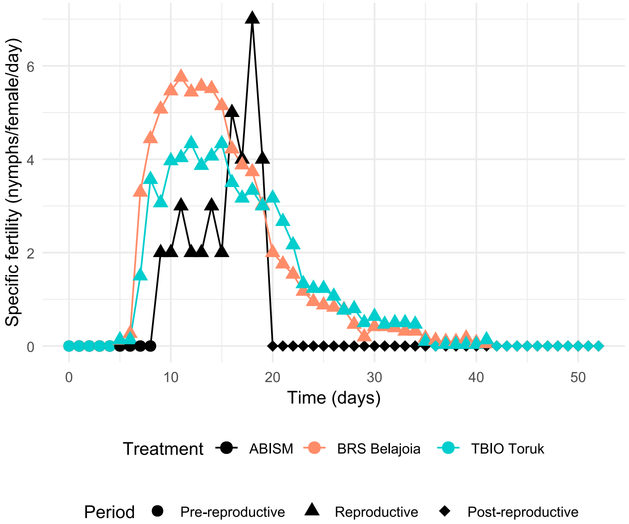

Fig. 4 Nymphs per female per day produced by *Rhopalosiphum padi* on wheat cv. BRS Belajoia and cv. TBIO Toruk under laboratory conditions (20±1°C, 12 h photoperiod), compared to values simulated by the ABISM model

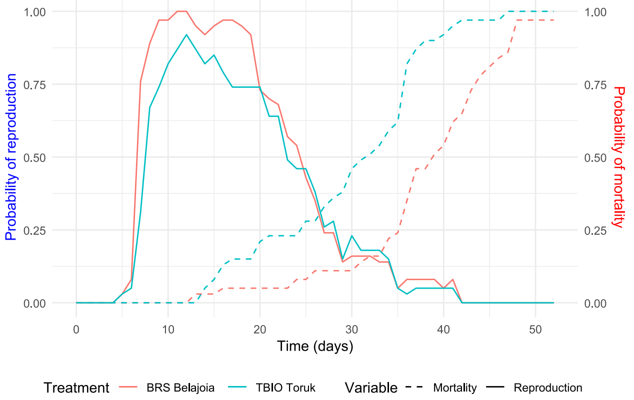

Fig. 5 Probability curves of reproduction and mortality of *Rhopalosiphum padi* on two wheat cultivars under controlled conditions (20±1°C, 12 h photoperiod) during 52 days

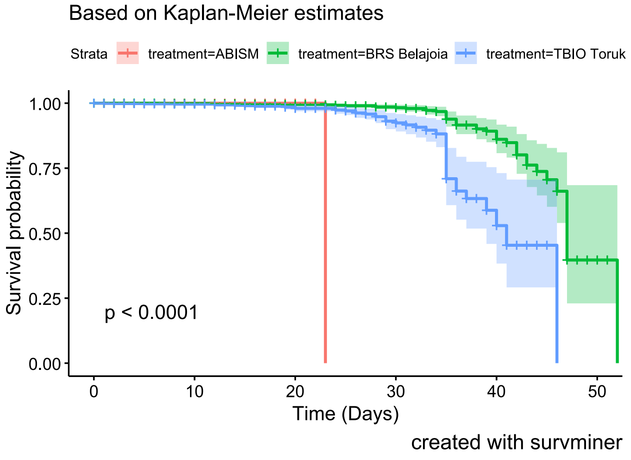

Fig. 6 Survival probability of *Rhopalosiphum padi* on two wheat cultivars under controlled conditions (20±1°C, 12 h photoperiod), compared to that predicted by the ABISM model

For the fertility curve simulated by ABISM, lower natality was observed during the first 16 days, followed by a sharp increase reaching eight nymphs/day, and then an abrupt decline.

Regarding reproductive likelihood over time, the curves showed a similar pattern between the cultivars (Fig. 5). However, during the initial phase—when reproduction increased until reaching the peak and then stabilized (between 8 and 20 days)—BRS Belajoia exhibited a higher reproductive rate than TBIO Toruk. In the declining phase, between 21 and 35 days, TBIO Toruk maintained a slightly higher reproductive rate. Mortality remained consistently higher in TBIO Toruk, equaling that of BRS Belajoia only at 50 days, when the maximum probability of death was reached.

The survival curves obtained by Kaplan–Meier estimates were distinct between cultivars (Fig. 6). Survival probabilities were similar among cv. BRS Belajoia, cv. TBIO Toruk, and ABISM until approximately 23 days. At this point, in a simulation under a fixed 20°C regime, the aphid agents in ABISM reached the defined thermal sum, resulting in

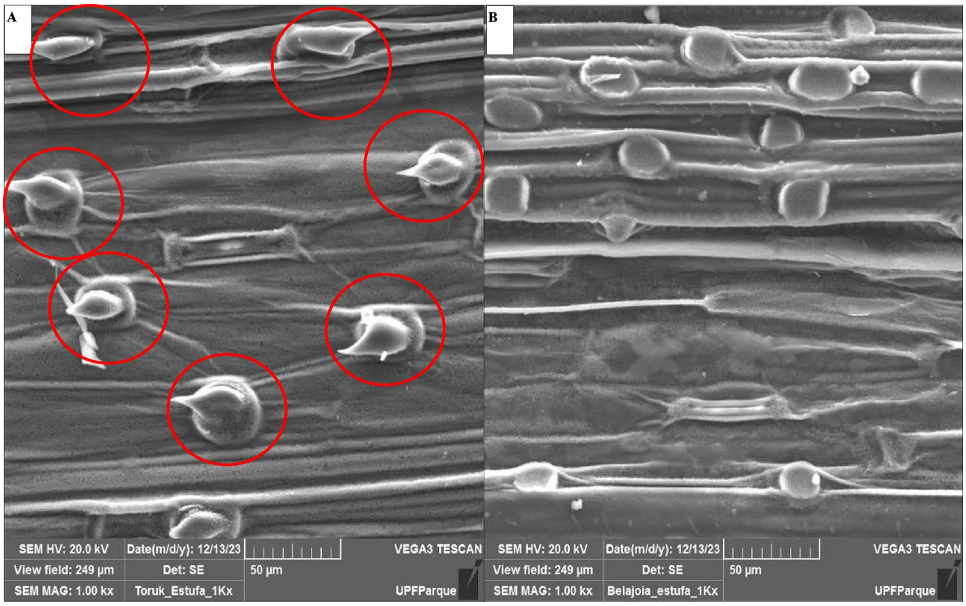

Fig. 7 Scanning electron microscope of the leaf epidermis of wheat cultivars TBIO Toruk (**A**) and BRS Belajoia (**B**)

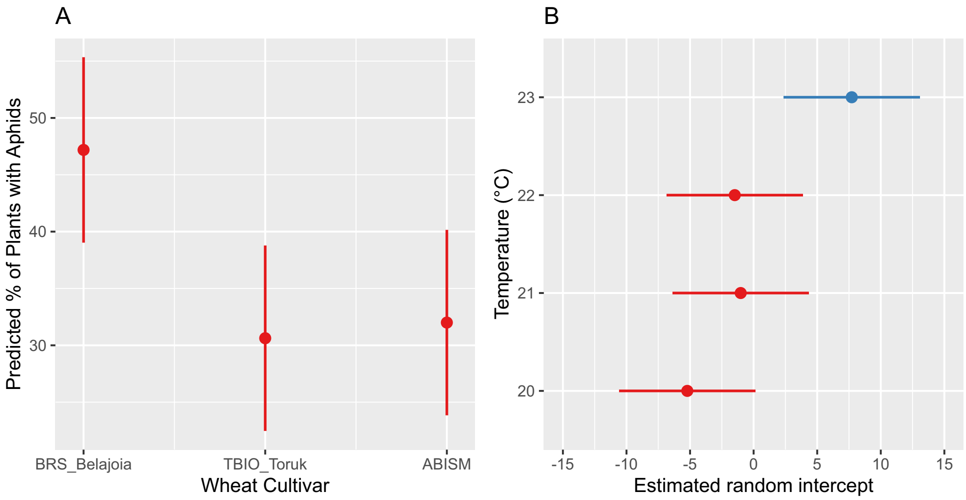

Fig. 8 Effects of host and temperature on the percentage of plants with aphids: **A** Effects of the two wheat cultivars and the ABISM model, represented in red. A significant difference ($p < 0.05$) was observed between BRS Belajoia (higher incidence) and the other treatments, whereas TBIO Toruk and ABISM did not differ; **B** Estimate of the random effects of temperature, where blue bars indicate positive values and red bars indicate negative values in relation to zero

the "death" event. Comparing the cultivars, aphid survival probabilities began to diverge at 25 days, when the confidence intervals of cv. TBIO Toruk diverged from the curve of cv. BRS Belajoia. Survival probability in cv. TBIO Toruk declined more rapidly, reaching zero at 45 days (death of the last individual). In contrast, in cv. BRS Belajoia, survival probability remained higher for longer, reaching zero only at 52 days (death of the last individual).

To investigate morphological traits differing between cultivars that could be associated with variations in the development, reproduction, and mortality of *R. padi*, we observed the wheat leaf epidermis using SEM. The most evident distinctive trait was the presence of trichomes only in cv. TBIO Toruk (A). In cv. BRS Belajoia (B), only structures resembling trichome bases were observed (Fig. 7).

Population growth and dispersal

Further corroborating the hypotheses of this study, the host-driven differences in the aphid's biological parameters were reflected in the spatiotemporal dynamics of *R. padi*. There were effects of the cultivar factor (Fig. 8A) and the temperature factor (Fig. 8B) on the percentage of plants infested by *R. padi*. The cv. BRS Belajoia, associated with higher longevity and fecundity, showed a significantly higher infestation ($\bar{x} = 47\%$) compared to cv. TBIO Toruk ($\bar{x} = 31\%$). With increasing mean temperature, the number of infested plants also increased. The relationship between infestation and temperature for the two cultivars was as follows: for cv. BRS Belajoia, 33–45% at 20°C, 23–57% at 21°C, 35–49% at 22°C, and 55–78% at 23°C; for cv. TBIO Toruk, infestation ranged from 9–26% at 20°C, 20–59% at 21°C, 18–41% at 22°C, and 25–58% at 23°C.

Thus, temperature and cultivar factors affected the probability of plants being infested by aphids (Fig. 9). Infestation probabilities increased with higher temperatures. In cv. TBIO Toruk, 17% of plants exceeded a 50% infestation likelihood at 20°C, growing to 52% at 23°C. In contrast, for cv. BRS Belajoia, the corresponding values were 53% at 20°C and 91% at 23°C.

The simulation in the ABISM model, using a fixed temperature regime, predicted an increase in aphid infestation with rising temperatures between 5°C and 25°C. The percentage of infested plants started at 9% at 5°C, increased to 15–20% between 10°C and 15°C, and reached 41% at 25°C (Fig. 10). Within the temperature range of the trials (20–23° C), the model more closely matched the results for cv. TBIO Toruk, while it underestimated the number of infested plants for cv. BRS Belajoia.

Discussion

Rhopalosiphum padi exhibited superior biological parameters when maintained on cv. BRS Belajoia compared to cv. TBIO Toruk. The number of nymphs established on cv. BRS Belajoia was higher than on cv. TBIO Toruk. They also reached the reproductive period earlier and had a higher birth rate during the initial days of this phase of their life cycle. Consequently, total fecundity was greater. Aphid longevity was also higher on cv. BRS Belajoia. Together, these

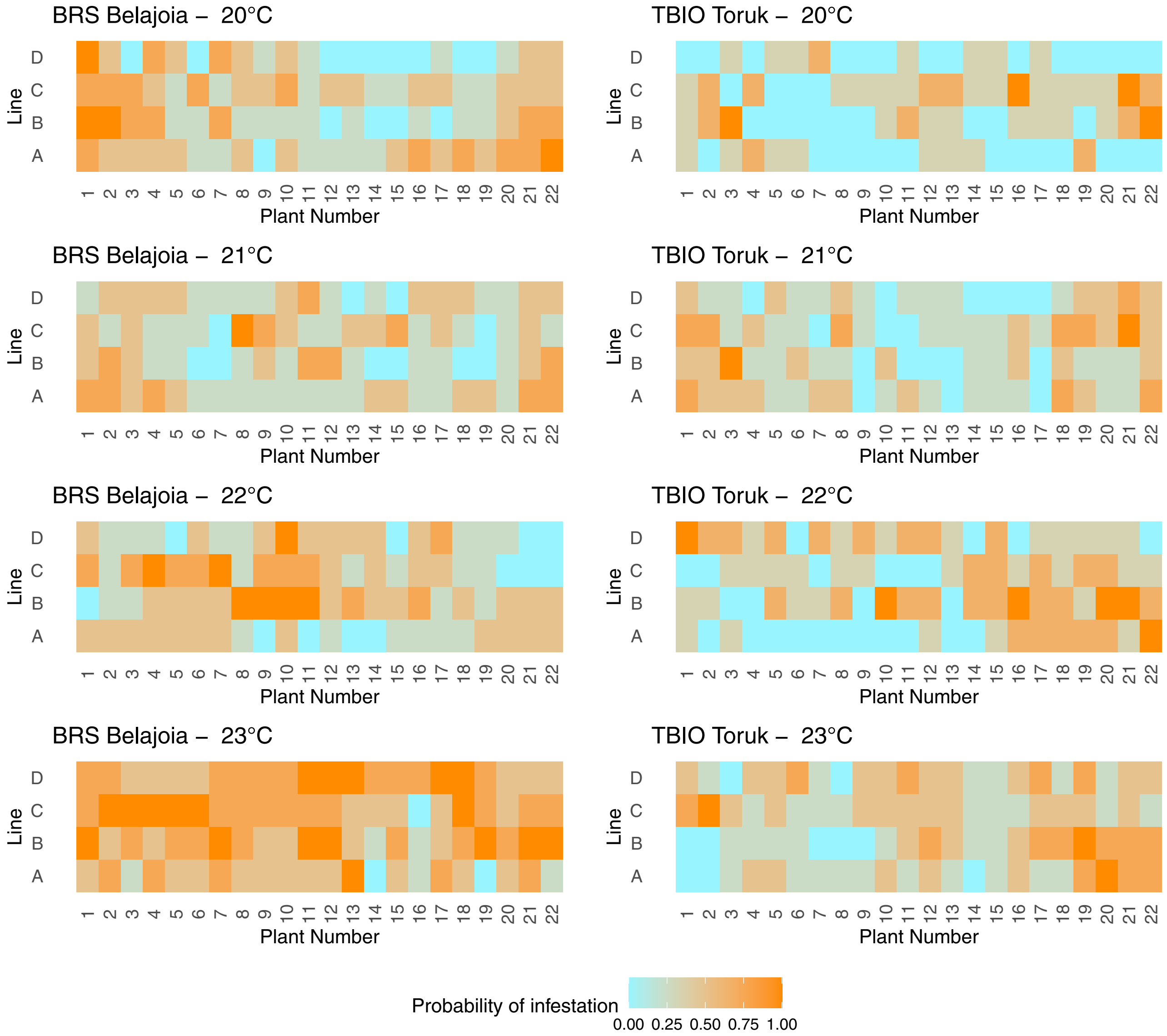

Fig. 9 Infestation probability of aphids on plants of two wheat cultivars during four exposure periods with mean temperatures ranging from 20 to 23°C

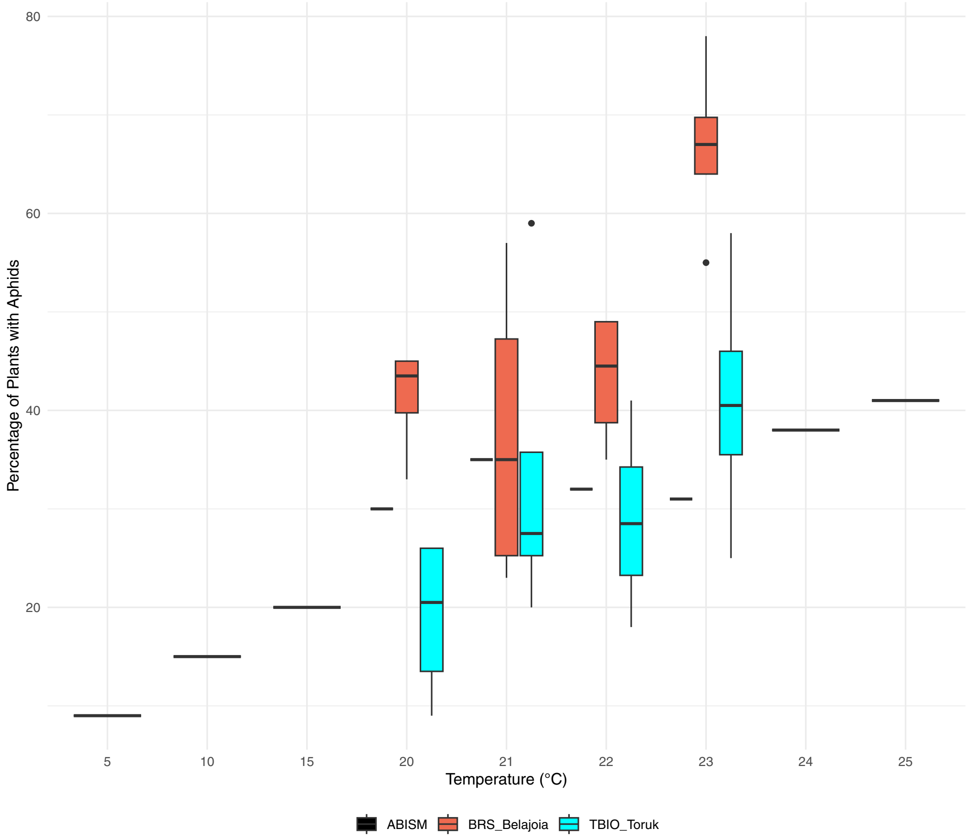

Fig. 10 Percentage of plants with aphids as a function of temperature and wheat cultivar in relation to the simulation of the ABISM model under a fixed temperature regime

Table 2 Comparison of different studies on biological parameters of aphids, including total number of nymphs born, nymphs born per day, longevity, and observations for various wheat and barley cultivars at different temperatures

Study	Fecundity nymphs/female	Specific fertility nymphs/ female/day	Longevity (days)	Observations
Present study	70.7	4.1	37.4	Wheat (cv. BRS Belajoia, 20°C, pre-reproductive duration: 7.2 days)
Present study	50.9	3.5	29.1	Wheat (cv. TBIO Toruk, 20°C, pre-reproductive duration: 8.4 days)
Present study, ABISM model	36.0	3.3	21.0	Wheat (cv. Embrapa 16, 20°C, pre-reproductive duration: 7.0 days)
Descamps and Chopa (2011)	39.6	2.0	16.6	Wheat (cv. Biointa), 24°C, pre-reproductive duration: 5.1 days
Rossa et al. (2017)			43.6±23.8	Wheat, 20°C, duration of nymphal period: 5.7–9.9 days
Park et al. (2017)	67.7	3.4	21.1	Barley, 20°C
Pereira et al. (2016)	65.4	2.5	46.2	Wheat (cv. Embrapa 16), 20°C, pre-reproductive duration: 7.2 days
Pereira et al. (2016)	57.8	2.4	40.2	Wheat (cv. BRS Timbauva), 20°C, pre-reproductive duration: 6.8 days
Singh et al. (2020)	±72.0			Wheat (cv. Solstice), 20°C
Singh et al. (2020)	±65.0			Wheat (cv. W 591), 20°C
Singh et al. (2020)	±55.0			Wheat (cv. W 068), 20°C
Singh et al. (2020)	±55.0			Wheat (cv. W 064), 20°C

parameters suggest that cv. BRS Belajoia is a higher-quality host for *R. padi* compared to cv. TBIO Toruk.

The biological parameters obtained in this study for *R. padi* fall within the range of variation and/or are close to the values reported in other studies (Table 2). For example, Park et al. (2017), studying barley at 20°C, reported a total fecundity of 67.7 nymphs. This is consistent with the 70.7 nymphs observed on cv. BRS Belajoia, but notably higher than the 50.9 recorded on cv. TBIO Toruk. Their reported specific fertility (3.4 nymphs/female/day) aligns closely with cv. TBIO Toruk (3.5), though it remains lower than that of cv. BRS Belajoia (4.1). Regarding longevity, Park et al. (2017) observed 21.1 days, a value considerably shorter than the lifespans reached on cultivars BRS Belajoia (37.4 days) and TBIO Toruk (29.1 days). Descamps and Chopa (2011) observed a specific fertility of 2.0 nymphs/female/day in wheat cv. Biointa at 24°C, with a longevity of 16.6 days and a total fecundity of 39.6 nymphs. Taken together, and as previously pointed out by Rossa et al. (2017), these results demonstrate that the life cycle rates of *R. padi* are significantly influenced by the host, exhibiting both interspecific and intraspecific variation.

Although this study did not focus on investigating resistance mechanisms, the distinct roughness of cv. TBIO Toruk leaves prompted an analysis of the epidermal surface. Microscopic evaluation confirmed the presence of prominent trichomes in TBIO Toruk, which were absent in cv. BRS Belajoia. While these morphological traits may function as physical barriers, they could also play a chemical role, as trichomes can release toxic compounds or sticky exudates that hinder insect movement (Peter et al. 1995; Porta and Rocha-Sosa 2002; de Jesus et al. 2020; Singh et al. 2021, 2022). However, it is important to note that the observed resistance in TBIO Toruk may not be exclusively attributed to these structures. Recent studies suggest that aphid performance may depend more heavily on the accessibility and quality of phloem composition rather than structural traits (Nalam et al. 2021), or that chemical defenses, such as benzoxazinoids, play a more significant role than trichomes (Batyrshina et al. 2020). Therefore, while the presence of trichomes is a clearly distinguishing feature, it likely represents only one component of a broader, multifactorial suite of resistance mechanisms in TBIO Toruk.

A primary goal of this study was to quantify how the host (wheat cultivar) influences aphid biological parameters and, consequently, the predictive accuracy of the ABISM model. Our results reveal that while the parameters defined in ABISM show varying degrees of alignment with the literature, they frequently diverge from the empirical data obtained for specific cultivars. Regarding total fecundity, ABISM's default value (36.0 nymphs) was notably lower than those observed on cvs. BRS Belajoia (70.7) and TBIO Toruk (50.9), as well as the 67.7 nymphs reported by Park et al. (2017) This indicates that the model significantly underestimates the reproductive potential of *R. padi* on these wheat materials.

In contrast, the model's specific fertility (3.3) demonstrated high consistency with the literature (3.4) and cv. TBIO Toruk (3.5), although it still underestimated the performance seen on cv. BRS Belajoia (4.1). A similar pattern was observed for longevity: while ABISM's value (21 days) closely mirrored the 21.1 days reported by Park et al. (2017), it failed to capture the significantly extended lifespans supported by the cultivars in this study, which reached up to 37.4 days on BRS Belajoia. These discrepancies suggest that the 'average' parameters typically used in modeling studies may compromise accuracy when applied to high-performance hosts, highlighting the need for cultivar-specific calibrations to improve spatiotemporal predictions.

The discrepancies observed between the experimental biological data and the model's predictions are also closely linked to the internal structure and established rules of ABISM. This is particularly evident regarding mortality logic. To address these limitations and improve model refinement, we specifically recommend a transition from deterministic to stochastic mortality rules within the ABISM framework. Currently, the model employs a threshold-based mortality where all aphid agents die upon reaching a predefined thermal sum (accumulated degree-days). To better reflect biological reality, we propose implementing a daily survival probability that decreases as the organism progresses through its life cycle. Instead of a fixed terminal point, mortality would be modeled as a cumulative risk function, allowing for a natural distribution of longevities within the population. This modification would prevent artificial population crashes in the simulation and more accurately capture the overlapping generations and gradual senescence observed on high-performance hosts, such as cv. BRS Belajoia.

The findings of this study also provide strong empirical support for the hypothesis that host-specific biological parameters significantly dictate the spatiotemporal dynamics of *R. padi*. The divergence in life-history traits between the two cultivars translated directly into contrasting infestation levels across the temperature gradient. While cv. BRS Belajoia supported high infestation rates, reaching a peak of 55–78% at 23°C, cv. TBIO Toruk consistently exhibited lower population pressure, with infestation ranging from only 9–26% at 20°C and peaking at a more modest 25–58% at 23°C. These results demonstrate that the 'host plant effect' acts as a primary filter for the potential growth of the pest; even as temperatures increased—typically a driver for aphid proliferation—the resistance mechanisms in TBIO Toruk (likely linked to the previously discussed morphological and chemical traits) prevented the infestation from reaching the high levels seen in the more susceptible BRS Belajoia. Consequently, using generalized parameters in predictive models without accounting for cultivar resistance would lead to significant overestimations of risk in resistant materials and potential underestimations in susceptible ones. Therefore, our data confirm that the interaction between the host genotype and biological parameters is a

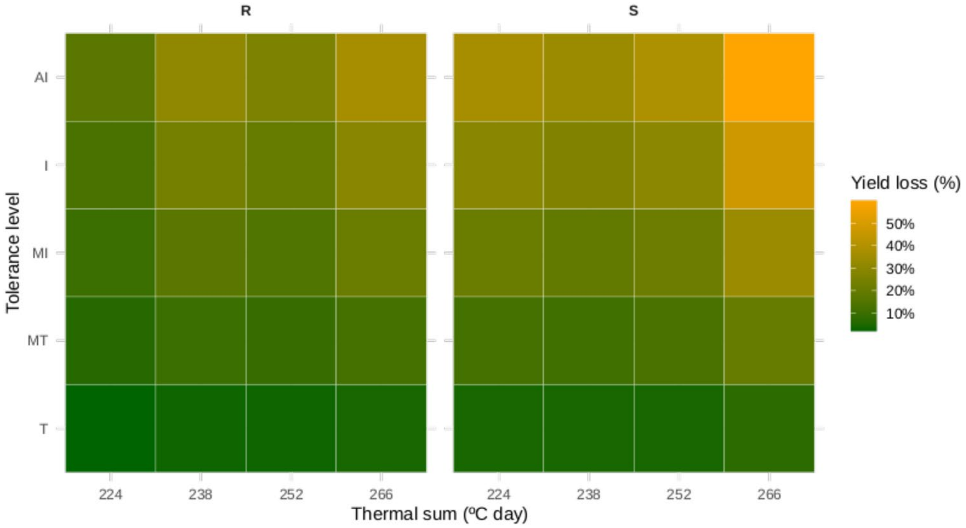

Fig. 11 Estimated yield loss (%) in wheat as a function of thermal sum (accumulated degree-days), aphid resistance (S = susceptible; R = resistant), and BYDV tolerance. BYDV tolerance classes: AI = Highly Intolerant; I = Intolerant; MI = Moderately Intolerant; MT = Moderately Tolerant; T = Tolerant

critical determinant of pest spatial dynamics and, by extension, the predictive accuracy of spatiotemporal models.

Finally, we explore the consequences of host resistance and its impacts on spatiotemporal dynamics, estimated grain yield, and subsequent management strategies. Direct damages from *R. padi* include reductions in spikes, tillers, dry mass, and overall grain yield (Roza-Gomes et al. 2008), while indirect damages involve the transmission of viruses such as BYDV-PAV (Lau et al. 2021a). Interestingly, the two cultivars analyzed exhibit antagonistic traits regarding insect resistance and viral tolerance. Cv. BRS Belajoia is moderately tolerant to BYDV-PAV (≈ 30% loss) but highly susceptible to the vector, leading to a higher number of infested plants. In contrast, cv. TBIO Toruk is more resistant to the aphid but moderately intolerant to the virus, with potential losses reaching 56%. When these factors are integrated, the estimated final impact on grain yield converges to surprisingly similar values. For instance, under high-temperature scenarios, the 91% infestation probability projected for BRS Belajoia results in a 27% yield reduction. Conversely, TBIO Toruk, despite a lower infestation probability (52%), faces a similar 29% reduction due to its lower viral tolerance (Lau et al. 2021a). To demonstrate this broader impact, we projected losses across five BYDV tolerance classes based on accumulated degree-days (°C day) and host resistance. Within a 14-day interval at 23° C, potential losses ranged from 10% for resistant/tolerant materials to 50% for those susceptible to both the vector and the virus (Fig. 11). These findings emphasize that management decisions cannot rely solely on aphid population thresholds; they must integrate the specific synergy between host-vector resistance and host-pathogen tolerance to accurately mitigate grain yield losses.

The findings of this study provide compelling evidence that aphid population growth models must incorporate host-specific biological parameters to accurately predict spatiotemporal dynamics, grain yield losses, and to support effective management decision-making. Our results reveal that the ABISM model, and similar predictive frameworks, achieve significantly greater accuracy when their internal rules explicitly account for insect–host interactions, such as those observed between cultivars with varying levels of resistance. Regarding model refinement, we propose a shift from generalized parameters toward the creation of resistance classes. By grouping cultivars with similar life-history traits—such as nymph survival, developmental rates, and fecundity—models can be calibrated more efficiently without losing biological resolution. In this context, the data obtained from cv. BRS Belajoia could define a “susceptible” group characterized by high reproductive potential and extended longevity, while cv. TBIO Toruk would represent a “resistant” group where morphological or chemical barriers constrain pest proliferation. Furthermore, we recommend transitioning from deterministic mortality thresholds to stochastic, daily survival probabilities. This structural improvement, combined with cultivar-specific data on daily nymph production and reproductive periods, would prevent artificial population crashes and better capture the overlapping generations essential for simulating real-world outbreaks. Ultimately, integrating these host-driven biological nuances is a critical step toward transforming simulation models from theoretical tools into precise instruments for integrated pest management (IPM) in wheat systems.

Conclusion

This study corroborates that host-specific interactions significantly dictate aphid biological parameters, directly impacting the spatiotemporal dynamics and predictive accuracy of the ABISM model. By quantifying these variations, we demonstrate that integrating "resistance classes" into simulation frameworks is a vital practical tool for refining pest forecasting. Consequently, transitioning from generalized rules to cultivar-specific mortality and reproduction data is essential to reduce discrepancies in grain yield loss estimates. Ultimately, these biological refinements transform predictive models into precise instruments for strategic decision-making in IPM.

Acknowledgements Rafael Rieder acknowledges the Brazilian National Council for Scientific and Technological Development (CNPq) for the Productivity Research Fellowship in Technological Development and Innovative Extension (DT).

Author Contributions Conceptualization: Talison Roberto Maurer, Douglas Lau. Data curation: Talison Roberto Maurer. Formal analysis: Talison Roberto Maurer, Douglas Lau. Funding acquisition: Douglas Lau, Rafael Rieder. Investigation: Talison Roberto Maurer, João Pedro Moretti, Mateus Riva Donati. Methodology: Talison Roberto Maurer, Rafael Rieder, Douglas Lau. Project administration: Rafael Rieder, Douglas Lau. Resources: Talison Roberto Maurer, João Pedro Moretti, Mateus Riva Donati. Software: Talison Roberto Maurer, Jose Mauricio Cunha Fernandes, Alexandre Tagliari Lazzaretti, Roberto Wiest, Rafael Rieder. Supervision: Rafael Rieder, Douglas Lau. Validation: Talison Roberto Maurer, Crislaine Sartori Suzana-Milan, Douglas Lau. Visualization: Talison Roberto Maurer. Writing—original draft: Talison Roberto Maurer. Writing—review & editing: Talison Roberto Maurer, Rafael Rieder, Douglas Lau.

Funding The Article Processing Charge (APC) for the publication of this research was funded by the Coordenação de Aperfeiçoamento de Pessoal de Nível Superior - Brasil (CAPES) (ROR identifier: 00x0ma614). This research was partially supported by the Brazilian National Council for Scientific and Technological Development (CNPq), processes 403878/2021-7 (Douglas Lau) and 302773/2022-3 (Rafael Rieder). Talison Roberto Maurer was financed in part by the Coordenação de Aperfeiçoamento de Pessoal de Nível Superior—Brasil (CAPES)—Finance Code 001.

Declarations

Conflict of interest The authors declare that they have no conflict of interest or other interests that might be perceived to influence the results and/or discussion reported in this paper.

Ethics approval and consent to participate Not applicable.

References

Aradottir GI, Crespo-Herrera L (2021) Host plant resistance in wheat to barley yellow dwarf viruses and their aphid vectors: a review. Curr Opin Insect Sci 45:59–68. https://doi.org/10.1016/j.cois.2021.01.002

Auad AM, Alves SO, Carvalho CA et al (2009) The impact of temperature on biological aspects and life table of Rhopalosiphum padi (Hemiptera: Aphididae) fed with signal grass. Fla Entomol 92:569–577. https://doi.org/10.1653/024.092.0406

Barlow N, Dixon A (1980) Simulation of lime aphid population dynamics. Centre for Agricultural Publishing and Documentation

Bates D, Mächler M, Bolker B et al (2015) Fitting linear mixed-effects models using lme4. J Stat Softw. https://doi.org/10.18637/jss.v067.i01

Batyrshina ZS, Yaakov B, Shavit R et al (2020) Comparative transcriptomic and metabolic analysis of wild and domesticated wheat genotypes reveals differences in chemical and physical defense responses against aphids. BMC Plant Biol 20:19. https://doi.org/10.1186/s12870-019-2214-z

Brabec M, Hončk A, Pekár S et al (2014) Population dynamics of aphids on cereals: digging in the time-series data to reveal population regulation caused by temperature. PLoS ONE 9:e106228. https://doi.org/10.1371/journal.pone.0106228

Correa LDJ, Maciel OVB, Bücker-Neto L et al (2020) A comprehensive analysis of wheat resistance to Rhopalosiphum padi (Hemiptera: Aphididae) in Brazilian wheat cultivars. J Econ Entomol 113:1493–1503. https://doi.org/10.1093/jee/toaa059

D'agostini M (2021) Regulação da população do afídeo Rhopalosiphum padi por predadores e parasitoides em cereais no norte do Rio Grande do Sul: abordagem por meio de modelo baseado em agente. Universidade de Passo Fundo,(Master's thesis)

Descamps LR, Chopa CS (2011) Population growth of *Rhopalosiphum padi* L. (Homoptera: Aphididae) on different cereal crops from the semiarid pampas of Argentina under laboratory conditions. Chil J Agric Res 71:390–394. https://doi.org/10.4067/S0718-58392011000300007

dos Santos CDR, Lau D, Redaelli LR et al (2022) Aphid-parasitoids trophic relationship in a cereal crop succession system: population oscillation and food webs. Agric For Entomol 24:516–530. https://doi.org/10.1111/afe.12513

El-Fatih M, Mohammad A, Shehawy A (2015) Biological aspects and thermal requirements of the bird cherry-oat aphid, *Rhopalosiphum padi* (Linnaeus), reared on wheat seedlings. J Plant Prot Pathol 6:1663–1670. https://doi.org/10.21608/jppp.2015.75784

Engel E, Lau D, Godoy WAC et al (2022) Oscillation, synchrony, and multi-factor patterns between cereal aphids and parasitoid populations in southern Brazil. Bull Entomol Res 112:143–150. https://doi.org/10.1017/S0007485321000729

Girvin J, Whitworth RJ, Rojas LMA et al (2017) Resistance of select winter wheat (*Triticum aestivum*) cultivars to *Rhopalosiphum padi* (Hemiptera: Aphididae). J Econ Entomol 110:1886–1889. https://doi.org/10.1093/jee/tox164

Hernandez-Ochoa I, Asseng S (2018) Cropping systems and climate change in humid subtropical environments. Agronomy 8:19. https://doi.org/10.3390/agronomy8020019

Hesler LS (2005) Resistance to *Rhopalosiphum padi* (Homoptera: Aphididae) in three triticale accessions. J Econ Entomol 98:603–610. https://doi.org/10.1603/0022-0493-98.2.603

Hothorn T, Bretz F, Westfall P (2008) Simultaneous inference in general parametric models. Biom J 50:346–363. https://doi.org/10.1002/bimj.200810425

Joris HAW, Penckowski LH, Kuhnem P, et al (2022) Informações técnicas para trigo e triticale: 14^a reunião da comissão brasileira de pesquisa de trigo e triticale. Tech. rep., Fundação ABC e Biotrigo

Genética. https://www.conferencebr.com/conteudo/arquivo/informacoes-tecnicas-para-trigo-e-triticale-safra-2022-1649081250.pdf

Kaplan EL, Meier P (1958) Nonparametric estimation from incomplete observations. J Am Stat Assoc 53:457–481. https://doi.org/10.1080/01621459.1958.10501452

Kassambara A, Kosinski M, Biecek P (2021) survminer: drawing survival curves using "ggplot2". cran.r-project.org/package=survminer

Kruskal WH, Wallis WA (1952) Use of ranks in one-criterion variance analysis. J Am Stat Assoc 47:583. https://doi.org/10.2307/2280779

Lau D, Mar TB, Castro R (2021a) Reação ao BYDV-PAV de cultivares de trigo do ensaio estadual do Rio Grande do Sul, em 2020. (Tech. rep., Embrapa Trigo)

Lau D, Mar TB, dos Santos CDR, et al (2021b) Advances in understanding the biology and epidemiology of barley yellow dwarf virus (BYDV). Achieving durable disease resistance in cereals. pp 709–745. https://doi.org/10.1201/9781003180715

Lau D, Mar TB, Silva FN, et al (2022) Barley yellow dwarf virus em trigo no Brasil. Revisão Anual de Patologia de Plantas. pp 216–239. https://doi.org/10.31976/0104-038321v280010

Leather SR, Dixon AFG (1981) The effect of cereal growth stage and feeding site on the reproductive activity of the bird-cherry aphid, *Rhopalosiphum padi*. Ann Appl Biol 97:135–141. https://doi.org/10.1111/j.1744-7348.1981.tb03006.x

Logan J, Wollkind D, Hoyt S et al (1976) An analytic model for description of temperature dependent rate phenomena in arthropods. Environ Entomol 5(6):1133–1140. https://doi.org/10.1093/ee/5.6.1133

Morgan D (2000) Population dynamics of the bird cherry-oat aphid, *Rhopalosiphum padi* (L.), during the autumn and winter: a modelling approach. Agric For Entomol 2:297–304. https://doi.org/10.1046/j.1461-9563.2000.00079.x

Nalam VJ, Han J, Pitt WJ et al (2021) Location, location, location: Feeding site affects aphid performance by altering access and quality of nutrients. PLoS ONE 16:e0245380. https://doi.org/10.1371/journal.pone.0245380

Parizoto G, Rebonatto A, Schons J et al (2013) Barley yellow dwarf virus-PAV in Brazil: seasonal fluctuation and biological characteristics. Trop Plant Pathol 38:11–19. https://doi.org/10.1590/S1982-56762013000100002

Park CG, Choi BR, Cho JR et al (2017) Thermal effects on the development, fecundity and life table parameters of *Rhopalosiphum padi* (Linnaeus) (Hemiptera: Aphididae) on barley. J Asia Pac Entomol 20:767–775. https://doi.org/10.1016/j.aspen.2017.05.004

Pds P, Lau D, Júnior M, A (2016) Considerações sobre o manejo do complexo afídeos/viroses em trigo. Reunião da Comissão Brasileira de Pesquisa de Trigo e Triticale

Peng X, Qiao X, Chen M (2017) Responses of holocyclic and anholocyclic Rhopalosiphum padi populations to low-temperature and short-photoperiod induction. Ecol Evol 7:1030–1042. https://doi.org/10.1002/ece3.2720

Pereira PRVS, Dossa CCK, Dossa AA, et al (2016b) Longevidade e prolificidade de *Rhopalosiphum padi* (L.)(Hemiptera: Aphididae) em duas cultivares de trigo sob diferentes temperaturas. Tech. rep., Embrapa Trigo, https://ainfo.cnptia.embrapa.br/digital/bitstream/item/153772/1/ID43887-2016CTO366.pdf

Peruzzo R, Salvadori JR, Pereira PRVS et al (2007) Wheat cultivars response to *Rhopalosiphum padi* infestation. Pesq Agrop Bras 42:1681–1685. https://doi.org/10.1590/S0100-204X2007001200003

Peter AJ, Shanower TG, Romeis J (1995) The role of plant trichomes in insect resistance: a selective review. Phytophaga 7:41–63

Porta H, Rocha-Sosa M (2002) Plant lipoxygenases. physiological and molecular features. Plant Physiol 130:15–21. https://doi.org/10.1104/pp.010787

R Core Team (2024) R: A language and environment for statistical computing

Razmjou J, Mohamadi P, Golizadeh A et al (2012) Resistance of wheat lines to *Rhopalosiphum padi* (Hemiptera: Aphididae) under laboratory conditions. J Econ Entomol 105:592–597. https://doi.org/10.1603/EC11290

Rossa FRL, Giudici AC, Vasicek A et al (2017) *Rhopalosiphum padi* (L.) (Homoptera: Aphididae) on different wheat cultivars under laboratory conditions. Asian J Adv Agric Res 1:1–11. https://doi.org/10.9734/AJAAR/2017/33775

Roza-Gomes MF, Salvadori JR, Schons J (2008) Danos de *Rhopalosiphum padi* (L.) (Hemiptera: Aphididae) no trigo em função da duração e da densidade de infestação. Neotrop Entomol 37:577–581. https://doi.org/10.1590/S1519-566X2008000500013

Santos-Cividanes TM, Cividanes FJ, Souza LS et al (2022) Life tables of the ladybird beetles Harmonia axyridis, Cycloneda sanguinea and Hippodamia convergens reared on the greenbug Schizaphis graminum. Braz J Biol 82:e263276. https://doi.org/10.1590/1519-6984.263276

Savaris M, Lampert S, Salvadori JR et al (2013) Population growth and damage caused by *Rhopalosiphum padi* (L.) (Hemiptera, Aphididae) on different cultivars and phenological stages of wheat. Neotrop Entomol 42:539–543. https://doi.org/10.1007/s13744-013-0158-9

Shapiro SS, Wilk MB (1965) An analysis of variance test for normality (complete samples). Biometrika 52(3–4):591–611. https://doi.org/10.1093/biomet/52.3-4.591

Simon AL, Caulfield JC, Hammond-Kosack KE et al (2021) Identifying aphid resistance in the ancestral wheat Triticum monococcum under field conditions. Sci Rep 11:13495. https://doi.org/10.1038/s41598-021-92883-9

Singh B, Simon A, Halsey K et al (2020) Characterisation of bird cherry-oat aphid (*Rhopalosiphum padi* L.) behaviour and aphid host preference in relation to partially resistant and susceptible wheat landraces. Ann Appl Biol 177:184–194. https://doi.org/10.1111/aab.12616

Singh A, Dilkes B, Sela H et al (2021) The effectiveness of physical and chemical defense responses of wild emmer wheat against aphids depends on leaf position and genotype. Front Plant Sci 12:667820. https://doi.org/10.3389/fpls.2021.667820

Singh P, Arif Y, Miszczuk E et al (2022) Specific roles of lipoxygenases in development and responses to stress in plants. Plants 11:979. https://doi.org/10.3390/plants11070979

Strażyński P, Ruszkowska M (2015) The life cycle functional response of *Rhopalosiphum padi* (L.) to higher temperature: territorial expansion of permanent parthenogenetic development as a result of warmer weather conditions. J Plant Prot Res 55:162–165. https://doi.org/10.1515/jppr-2015-0021

Thackray DJ, Diggle AJ, Jones RAC (2009) BYDV PREDICTOR: a simulation model to predict aphid arrival, epidemics of barley yellow dwarf virus and yield losses in wheat crops in a Mediterranean-type environment. Plant Pathol 58:186–202. https://doi.org/10.1111/j.1365-3059.2008.01950.x

Villanuevab JR, Strong FE (1964) Laboratory studies on the biology of Rhopalosiphum padi (Homoptera: Aphidae). Ann Entomol Soc Am 57:609–613

Wickham H (2016) ggplot2. Springer International Publishing. https://doi.org/10.1007/978-3-319-24277-4

Wickham H, Averick M, Bryan J et al (2019) Welcome to the tidyverse. J Open Sour Softw 4:1686. https://doi.org/10.21105/joss.01686

Wiest R, Salvadori JR, Fernandes JM et al (2021) Population growth of Rhopalosiphum padi under different thermal regimes: an agent-based model approach. Agric For Entomol 23:59–69. https://doi.org/10.1111/AFE.12404

Zadoks JC, Chang TT, Konzak CF (1974) A decimal code for the growth stages of cereals. Weed Res 14:415–421. https://doi.org/10.1111/j.1365-3180.1974.tb01084.x